Journal of Alloys and Compounds 513 (2012) 353–358

Contents lists available at SciVerse ScienceDirect

Journal of Alloys and Compounds

journal homepage: www.elsevier.com/locate/jallcom

# Structural and magnetic properties of $CuCr_2Se_4$ single crystals diluted with Sb(III)

E. Malicka[a,*], A. Waśkowska[b], J. Heimann[c], R. Sitko[a], D. Kaczorowski[b]

[a] Chemistry Department, University of Silesia, Szkolna 9, 40-006 Katowice, Poland
[b] Institute of Low Temperature and Structure Research, Polish Academy of Sciences, P.O. Box 1410, 50-950 Wrocław, Poland
[c] Institute of Physics, University of Silesia, Uniwersytecka 4, 40-007 Katowice, Poland

ARTICLE INFO

*Article history:*
Received 7 August 2011
Received in revised form 17 October 2011
Accepted 18 October 2011
Available online 25 October 2011

*Keywords:*
Single crystals growth
X-ray diffraction
X-ray photoelectron spectroscopy
High $T_c$ ferromagnet
Magnetic measurements

ABSTRACT

A series of single crystals based on $CuCr_2Se_4$ spinel diluted with Sb ions was prepared by chemical vapour transport. They were characterized by X-ray fluorescent spectroscopy (XRF), X-ray diffraction, X-ray photoelectron spectroscopy (XPS) and bulk magnetization measurements. The results revealed that non-magnetic $Sb^{3+}$ ions substitute $Cr^{3+}$ ions at the octahedral sites. For the $Sb^{3+}$ content $x = 0.06$ the single crystals of $(Cu)[Cr_{2-x}Sb_x]Se_4$ were formed, while for larger Sb concentration ($x = 0.12$ and $x = 0.16$) the crystals with cation vacancies at the octahedral sites were obtained. The XPS data evidenced the $3d^3$ electronic configuration of Cr ions with localized magnetic moments for the three compositions differing in the Sb content. Despite the unaltered valence state of Cr ions along the series, the low-temperature magnetic characteristics have changed considerably. With increasing content of Sb the saturation magnetic moment was found to radically decrease. This effect may be explained in terms of the perturbation in the ferromagnetic Cr–Se–Cr indirect exchange interactions caused by the presence of increasing number of dopant atoms and vacancies in the crystal lattice.



## 1. Introduction

$CuCr_2Se_4$ is a ferromagnet exhibiting metallic conductivity. It has the cubic spinel structure with normal cation distribution and symmetry of the space group $Fd\bar{3}m$ [1–3]. The reported lattice parameter is in the range 10.321 Å [1]–10.337 Å [3]. The high Curie and paramagnetic Curie–Weiss temperatures of the range $T_c = 414.5$ K [1]–460 K [4–6] and $\theta_{CW} = 441$ K [7]–465 K [4,8], respectively, have been attributed to the strong ferromagnetic interactions between the collinear spins of chromium ions. However, the saturation magnetic moment is $\mu_{sat} = 4.5\ \mu_B$/mole [1]–5.07 $\mu_B$/mole [4–6], instead of 6 $\mu_B$/mole expected for two $Cr^{3+}$ ions [1,8]. This finding has been rationalized by the presence of the magnetic moment of about 1 $\mu_B$ with an opposite orientation [10–15]. The metallic conductivity of $CuCr_2Se_4$ has been accounted for delocalised charge carriers [16]. Its p-type character has been deduced from the positive value of the Seebeck coefficient [4–9].

Numerous experimental and theoretical studies, aimed at determining the electronic structure and magnetic behaviour of the parent phase $CuCr_2Se_4$ [4,5,10,12,17–19] and of the spinels admixed with $Ga^{3+}$[20–23], $In^{3+}$ [24,25] $Co^{2+}$[26,27], $Zn^{2+}$ [28,29] and $V^{3+}$ [30], have been published. Theoretical studies on magnetic phase diagrams for another system of diluted spinels $(Zn_{1-x}Cu_x)[Cr_2]Se_4$ with $0 \le x \le 1$ were described in [31]. Based on the mean field approximation those authors have shown for Cu concentration $x > 0.2$ the essential change in nature of magnetic interactions from antiferromagnetic to ferromagnetic.

The reported data guide a search for new materials with desired characteristics. However, the resulting opinions are still a subject of controversial discussions because the properties of these materials are very sensitive to even small changes in their chemical composition and crystal structure [9,12,15].

In the present paper we describe the effect of $Sb^{3+}$ admixture on the magnetic properties of the $CuCr_2Se_4$-based spinel. Three single crystals with different antimony concentration have been characterized by energy dispersive X-ray fluorescent spectroscopy (EDXRF) and X-ray diffraction technique in order to determine the crystal composition, cation distribution and stability of the cubic spinel structure. The X-ray photoelectron spectroscopy (XPS) data have been used to probe the electronic structure of the ions. The magnetic properties of the system have been investigated by means of magnetization measurements carried out in wide ranges of temperature and magnetic field strength.

## 2. Experimental

### 2.1. Synthesis

Single crystals of the $CuCr_2Se_4$ spinel admixed with Sb ions were grown from the mixture of the binary selenides CdSe and $Sb_2Se_3$ using a chemical vapour transport method with the anhydrous chromium chloride as a transporting agent. As the starting materials for the syntheses of the selenides were used high-purity

* Corresponding author. Tel.: +48 32 3591627.
*E-mail address:* ewa.malicka@us.edu.pl (E. Malicka).

0925-8388/$ – see front matter © 2011 Elsevier B.V. All rights reserved.
doi:10.1016/j.jallcom.2011.10.048

elements: cadmium, antimony and selenium, all with the stated purities better than 99.99%. The binary selenides were synthesized by solid state reaction in evacuated quartz ampoules. In the first step, the elements were heated at 873 K for 7 days. Subsequently, the materials were powderized, again sealed in quartz tubes and heated at 1073 K for 10 days. Phase analysis of the products was made by means of X-ray powder diffraction.

The crystal growth was carried out using stoichiometric amounts of the selenides and $CrCl_3$ in quartz ampoules (length ~200 mm, inner diameter $d$ = 20 mm) evacuated to about $\sim 10^{-3}$ Pa. Temperature of crystallization zone was between 923 and 953 K, while temperature of the melting zone was in the range 1013–1053 K. The obtained single crystals were of octahedral shape with well-formed regular (1 1 1) faces and edge lengths of about 1–3 mm.

The chemical composition of the crystals was determined using energy-dispersive X-ray fluorescence spectrometer (EDXRF) described in details in [32]. The results of are given in Table 1.

### 2.2. X-ray diffraction

Three single crystals of $CuCr_2Se_4$ doped with different $Sb^{3+}$ concentrations and dimensions given in Table 2 were chosen for the X-ray structure determination. The measurements were performed on a four-circle diffractometer, Xcalibur/CCD Oxford Diffraction, operating in $\kappa$ geometry and using graphite monochromated MoKα radiation. The intensity data were collected with $\omega$-scan technique and $\Delta\omega$ step of 1.0°. A set of 1200 images was taken in nine runs of exposures with different crystal orientations in the reciprocal space. The exposure time per one image was 30 s. Crystal and instrument stability were controlled by one image, selected as a standard and measured after each 50 images [33]. The intensity data were integrated and corrected for Lorentz and polarization effects with the CrysAlis RED software [34]. Numerical absorption correction based on crystal shape was applied [34]. The structure refinement was performed using the SHELXL-97 program package [35]. The crystal data and some details on the experimental conditions are summarized in Table 2, together with general results of the structure refinements.

### 2.3. X-ray photoelectron spectroscopy (XPS)

The XPS spectra of the spinels and of reference $Sb_2Se_3$ were obtained with a monochromated AlKα radiation using PHI 5700/660 Physical Electronic spectrometer. The spectrometer was equipped with a hemispherical mirror analyser providing an energy resolution of about 0.3 eV. The scale of binding energy was calibrated using the Fermi level of Ag (0 eV), peaks $4f_{7/2}$ of Au (84.0 eV), $3d_{5/2}$ of Ag (368.3 eV) and $2p_{3/2}$ of Cu (932.7 eV). The samples were scarped *in situ* in $10^{-10}$ hPa vacuum in order to obtain free of contamination fresh surface. The following spectra have been measured: (1) an overview of the binding energy in the range −2 to 1400 eV; (2) the valence band in the region −2 to 20 eV, and (3) the core-level 107 characteristic peaks for Se: 3*d*, Cr and Cu: 2*p*; and Sb: 4*d*. The background was subtracted using the Tougaard's approximation. The intensities of the valence band and core-level characteristic peaks were normalized to the intensities of Se 4d peaks.

### 2.4. Magnetic measurements

Measurements of the magnetization were carried out on the samples freely placed in a sample holder. They were performed in the temperature range 1.71–500 K in applied magnetic fields of up to 5 T using a Quantum Design MPMS-5 superconducting quantum interference device (SQUID) magnetometer.

## 3. Results and discussion

### 3.1. Crystal structure and cation distribution

In the X-ray crystal structure calculations the origin of the unit cell was taken at the point $\bar{3}m$ of the space group $Fd\bar{3}m$ (no. 227). Assuming normal spinel structure, the Cu ions were placed in the tetrahedral (A) site 8*a*: (1/8, 1/8, 1/8), and the $Cr^{3+}$ ions in the octahedral [B] site 16*d*: (1/2, 1/2, 1/2). The Sb admixture was located in [B] sharing it with the Cr ions. The coupled site occupancy factors (SOF) and constrained atomic thermal displacements U of the two ions were treated as free variables. Because of strong correlation, the SOFs for Sb and Cr were refined separately in alternative runs of calculations. The convergence led to the acceptable atomic displacement parameters and SOFs, which allowed writing the chemical formula as given in Table 3. Similar procedure applied to Sb located in the (A) sites resulted in rejection of Sb from these positions. The refinement of SOF for Se in the site 32*e*: (*u*,*u*,*u*) gave the variability from the anion stoichiometry within the range of one

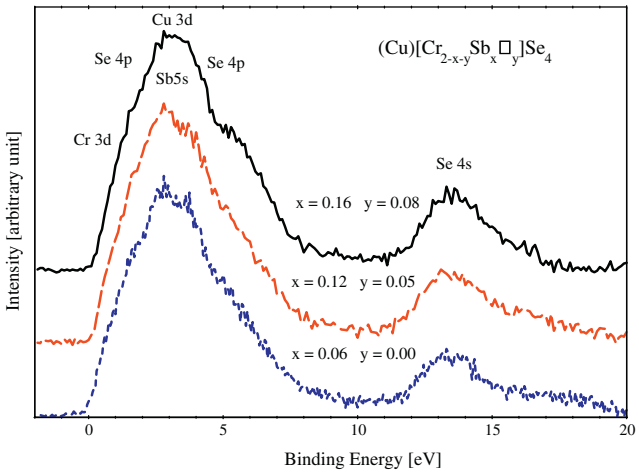


**Fig. 1.** XPS valence band spectra of the (Cu)[$Cr_{2-x-y}Sb_x\square_y$]$Se_4$ single crystals.

standard deviation in determination of this parameter. We assume however that some anion deficit cannot be excluded.

The obtained Sb concentration ($x < 0.20$) does not exceed a critical quantity for isomorphous substitution preserving the spinel structure. The attempts to grow single crystals with higher Sb concentration have not been successful. The dilution of the Cr-subarray in the present samples brings in a minor expansion of the unit cell that results from difference in the ionic radii of $Cr^{3+}$ (0.615 Å) and $Sb^{3+}$ (0.76 Å) ions (Table 4b). The Se positional parameter $u$ (Table 3) points to the slightly distorted $BSe_6$ octahedra (Table 4a). However, this parameter which is a measure of the anion sublattice distortion and controls the Cr–Se–Cr superexchange interactions, does not show any clear tendency in the three samples when compared to $u$ = 0.25756 [2] in the parent $CuCr_2Se_4$. It is interesting that in the crystals with $x$ = 0.12 and 0.16 a noticeable number of cationic vacancies at the octahedral sites have been observed. Thus, the chemical formula should be written as (Cu)[$Cr_{2-x-y}Sb_x\square_y$]$Se_4$, where □ denotes the vacancy. In the crystal with $x$ = 0.06 the vacancy concentration $y$ = 0, while in the crystals with $x$ = 0.12 and 0.16 the respective vacancies are $y$ = 0.05 and 0.08.

The bond distances and the bond angles are listed in Table 4a. Apparently, the Cu–Se distances are significantly shorter than the theoretical covalent and ionic bonds of 2.450 and 2.550 Å, respectively [35,36]. This suggests a deviation from the formal valences of Cu cations. Based on the relationship between the bond length and its strength (valence) one may calculate the Cu valences [37–39]. The calculations with the program described in [40] indicate a fractional valence $v$ = +1.612, 1.648, 1.60 in the (A) sites of the three crystals, respectively. Then, it can be assumed that the Cu states are strongly hybridised with the Se 4*p* states. The fractional valence of Cu induces a corresponding number of holes in the conduction band that explains the *p*-type electric conductivity in the (Cu)[$Cr_{2-x-y}Sb_x\square_y$]$Se_4$ spinels studied.

### 3.2. X-ray photoelectron spectra

The XPS valence band spectra (VB) of the (Cu)[$Cr_{2-x-y}Sb_x\square_y$]$Se_4$ spinels are shown in Fig. 1. All three spectra are similar in character, i.e. an increase in the Sb concentration causes no apparent change in the valence band. In the energy range from 0 to 8 eV, VB's are predominantly formed by the Cr 3*d* and Se 4*p* levels. In accordance with the literature data [41], close to the maximum at 2.8 eV appear also the Cu 3*d* states. Due to these states the VB peak occurs at a little lower energy if compared to that in $Zn_{1-x}Sb_xCr_{2-x/3}Se_4$ spinel system [42]. A shallow local minimum observed in the region 2.7 to 3.7 eV is due to the Se 4*p* levels. As may be inferred from Fig. 1, this

**Table 1**
The chemical composition of the single crystals of (Cu)[$Cr_{2-x-y}Sb_x\square_y$]$Se_4$ in % (m/m).

| Compounds | Cu | Cr | Sb | Se |
|---|---|---|---|---|
| (Cu)[$Cr_{1.94}Sb_{0.06}$]$Se_4$ | 13.1 ± 0.3 | 20.7 ± 0.4 | 1.5 ± 0.1 | 64.7 ± 0.8 |
| (Cu)[$Cr_{1.83}Sb_{0.12}\square_{0.05}$]$Se_4$ | 13.1 ± 0.3 | 19.4 ± 0.5 | 3.0 ± 0.1 | 64.5 ± 0.9 |
| (Cu)[$Cr_{1.76}Sb_{0.16}\square_{0.08}$]$Se_4$ | 13.2 ± 0.3 | 18.6 ± 0.5 | 4.0 ± 0.1 | 64.2 ± 0.9 |

**Table 2**
Crystal data, experimental details and structure refinements results for the single crystals of (Cu)[$Cr_{2-x-y}Sb_x\square_y$]$Se_4$.

| ***Crystal data*** | (Cu)[$Cr_{1.94}Sb_{0.06}$]$Se_4$ | (Cu)[$Cr_{1.83}Sb_{0.12}\square_{0.05}$]$Se_4$ | (Cu)[$Cr_{1.76}Sb_{0.16}\square_{0.08}$]$Se_4$ |
|---|---|---|---|
| Crystal system, space group | Cubic, $Fd\bar{3}m$ | Cubic, $Fd\bar{3}m$ | Cubic, $Fd\bar{3}m$ |
| Unit cell dimensions (Å) | | | |
| *a* | 10.335(1) | 10.339(1) | 10.343(1) |
| Volume (Å$^3$) | 1104.00(3) | 1105.12(3) | 1106.37(3) |
| *Z* | 8 | 8 | 8 |
| Calculated density (Mg/m$^3$) | 5.867 | 5.885 | 5.886 |
| Crystal size (mm) | 0.10 × 0.10 × 0.10 | 0.08 × 0.08 × 0.10 | 0.12 × 0.10 × 0.10 |
| **Data collection** | | | |
| Wavelength (Å) | 0.71073 | 0.71073 | 0.71073 |
| $2\theta_{max}$ for data collection | 80.35 | 80.31 | 80.28 |
| Limiting indices: *h* | −18, 12 | −18, 13 | −17, 17 |
| *k* | −18, 18 | −13, 17 | −18, 18 |
| *l* | −13, 18 | −18, 17 | −18, 13 |
| Reflections collected | 5427 | 5048 | 5336 |
| Reflections unique | 198 | 198 | 198 |
| Reflections >2$\sigma$ (*I*) | 169 | 170 | 179 |
| Absorption coefficient (mm$^{-1}$) | 34.07 | 34.13 | 34.14 |
| R(int) | 0.05(2) | 0.07(2) | 0.05(1) |
| **Refinement** | | | |
| Refinement method | | Full-matrix least-squares on $F^2$ | |
| Number of refined parameters | 10 | 10 | 10 |
| Goodness-of-fit on $F^2$ | 1.001 | 1.003 | 1.008 |
| Final R indices [I>2$\sigma$(I)] $R_1$ | 0.018 | 0.024 | 0.019 |
| $wR_2$ | 0.049 | 0.071 | 0.048 |
| Extinction coefficient | 0.0015(1) | 0.0011(1) | 0.00077(6) |
| Largest diff. peak and hole (eÅ$^{-3}$) | 0.91 and −0.094 | 1.22 and −0.89 | 0.97and −0.93 |

**Table 3**
Atomic coordinates and equivalent isotropic displacement parameters for the single crystals of (Cu)[$Cr_{2-x-y}Sb_x\square_y$]$Se_4$.

| Compound | Anion positional parameter: *u* | SOF in [B]site | | $U_{iso}$ (×10$^3$ Å$^2$) | | |
|---|---|---|---|---|---|---|
| | | Cr | Sb | Cu | Cr/Sb | Se |
| (Cu)[$Cr_{1.94}Sb_{0.06}$]$Se_4$ | 0.25741(2) | 0.970(4) | 0.031(2) | 10.5(2) | 7.2(2) | 7.0(1) |
| (Cu)[$Cr_{1.83}Sb_{0.12}\square_{0.05}$]$Se_4$ | 0.25697(3) | 0.915(6) | 0.058(3) | 10.6(2) | 7.6(3) | 7.5(2) |
| (Cu)[$Cr_{1.76}Sb_{0.16}\square_{0.08}$]$Se_4$ | 0.25750(2) | 0.880(6) | 0.079(2) | 11.5(2) | 9.3(2) | 8.9(1) |

*Note.* The atomic positions are as follows: Cu in (A) site: 8 *a* (1/8, 1/8, 1/8), Cr/Sb in [B] site:16 *d* (1/2, 1/2, 1/2) and Se anion site: 32*e* (*u*, *u*, *u*).

**Table 4**
(a) Selected interatomic distances [Å] and angles [°] for the single crystals of (Cu)[$Cr_{2-x-y}Sb_x\square_y$]$Se_4$. (b) Ionic and covalent atomic radii [35,36].

| | (Cu)[$Cr_{1.94}Sb_{0.06}$]$Se_4$ | (Cu)[$Cr_{1.83}Sb_{0.12}\square_{0.05}$]$Se_4$ | (Cu)[$Cr_{1.76}Sb_{0.16}\square_{0.08}$]$Se_4$ |
|---|---|---|---|
| A–Se | 2.3704(5) ×4 | 2.3632(6) ×4 | 2.3737(5) ×4 |
| B–Se | 2.5095(4) ×6 | 2.5147(4) ×6 | 2.5105(4) ×6 |
| Se–B–Se | 180.00(1) ×3 | 180.00(1) ×3 | 180.00(1) ×3 |
| Se–B–Se$^i$ | 93.44(1) ×6 | 93.23(1) ×6 | 93.60(1) ×6 |
| Se–A–Se | 109.47(0) ×6 | 109.47(0) ×6 | 109.47(0) ×6 |
| A–Se–B | 122.79(1) ×6 | 122.94(1) ×6 | 122.76(1) ×6 |

| | Atomic radii [Å] | |
|---|---|---|
| | Ionic | Covalent |
| $Cu^{2+}$ | 0.57 | 1.28 |
| $Cu^{1+}$ | 0.60 | |
| $Cr^{3+}$ | 0.615 | 1.24 |
| $Sb^{3+}$ | 0.76 | 1.41 |
| $Se^{2-}$ | 1.98 | 1.17 |

*Note. i:* 1/4 + *x*, *y* + 1/4, 1 − *z*.

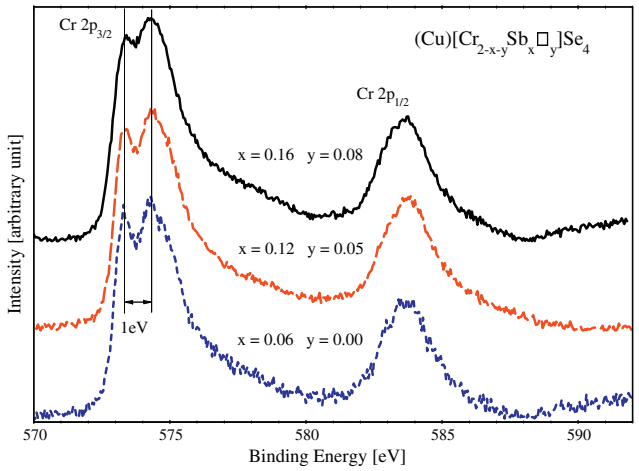


**Fig. 2.** XPS spectra of Cr 2*p* core-levels in the (Cu)[$Cr_{2-x-y}Sb_x\square_y$]$Se_4$ single crystals.

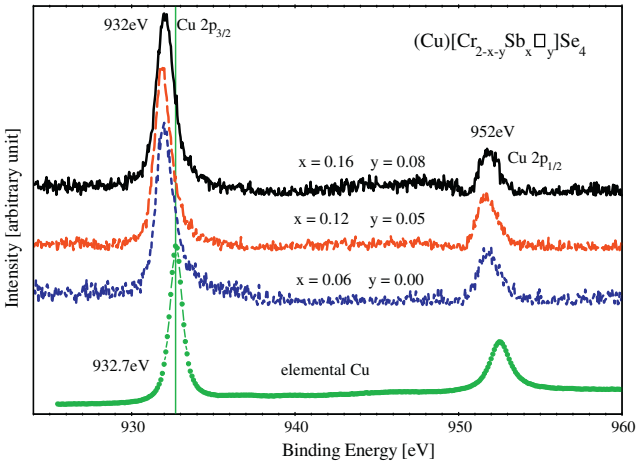


**Fig. 3.** XPS spectra of Cu 2*p* core-levels in the (Cu)[$Cr_{2-x-y}Sb_x\square_y$]$Se_4$ single crystals. The lowest curve corresponds to the elemental Cu.

dip becomes filled up with the Sb 5*s* levels when the Sb concentration increases. Far off the Fermi level, at the energy of 13.5 eV, are located the Se 4s states that seem to be affected by the increase of Sb admixture.

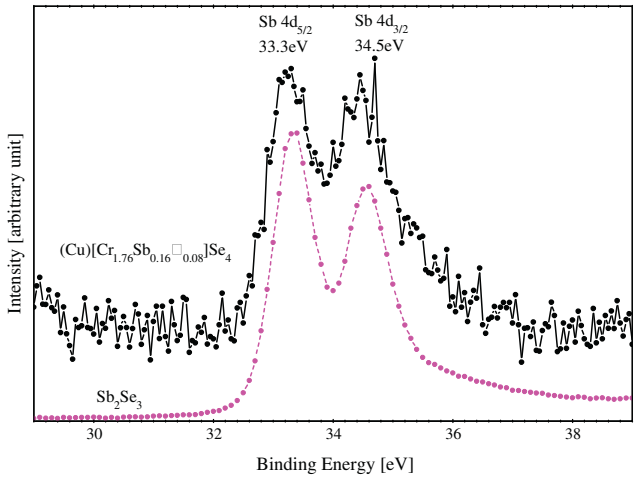


**Fig. 4.** XPS spectra of Sb 4*d* core-levels for (Cu)[$Cr_{1.76}Sb_{0.16}\square_{0.08}$]$Se_4$ single crystal and binary selenide $Sb_2Se_3$.

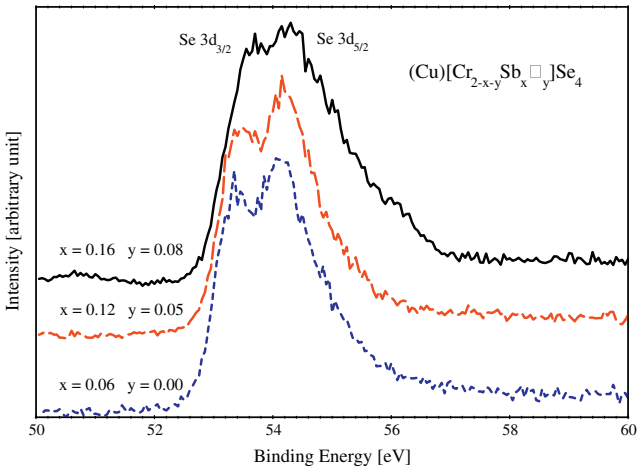


**Fig. 5.** XPS spectra of Se 3*d* core-levels in the (Cu)[$Cr_{2-x-y}Sb_x\square_y$]$Se_4$ single crystals.

Figs. 2–5 display the core levels in the (Cu)[$Cr_{2-x-y}Sb_x\square_y$]$Se_4$ compounds. The Cr *2p* spectra consisting of the Cr $2p_{3/2}$ doublet and the Cr $2p_{1/2}$ peak are shown in Fig. 2. The binding energy of the peaks is about 1 eV below the energy observed for the $Zn_{1-x}Sb_xCr_{2-x/3}Se_4$ system. The peaks of the Cr $2p_{3/2}$ doublet are at 573.3 eV and 574.3 eV, and the splitting originates from a coupling of the Cr $2p_{3/2}$ states and 3*d* Cr valence electrons [41]. Similar data were reported for the $Zn_{1-x}Sb_xCr_{2-x/3}Se_4$ system [42], $CuCr_2Se_4$ [41] and for a number of other chalcogenide spinels [43]. From *ab initio* calculations made for $Cr_2O_3$ it has been stated that the observed feature corresponds to the 3*d* elements with localized magnetic moment of 3 $\mu_B$ [44]. The experimental data indicated that the splitting of the $2p_{3/2}$ states can only be detected if the magnetic moments of the 3*d* elements are larger than 2 $\mu_B$, and the splitting is not observed for delocalised Cr states [43]. Besides, it was shown that the magnitude of the splitting is proportional to the local magnetic moment at the Cr site. Based on these observations we may conclude that in the (Cu)[$Cr_{2-x-y}Sb_x\square_y$]$Se_4$ series the Cr ions have the $3d^3$ electronic configuration. Though the positions of the two peaks seem insensitive to the Sb concentration, the dip between them becomes less pronounced when the amount of the Sb admixture increases. This effect is consistent with the results of structure determination, which locates the $Sb^{3+}$ ions at the octahedral positions of the cubic spinel, where they cause a perturbation in the periodicity of the chromium sublattices.

The Cu 2*p* core levels spectra are shown in Fig. 3. They display the spin-orbit components of the Cu $2p_{3/2}$ and Cu $2p_{1/2}$ doublet. Similar binding energy of the Cu $2p_{3/2}$ level was reported for CuSe and $Cu_2Se$ [45], and for $Cu_2SnSe_4$ [46]. The Cu $2p_{3/2}$ peaks are shifted by about 0.7 eV toward lower energy in relation to elemental copper (932.7 eV), that is consistent with chemical shift in the mentioned compounds. The energy difference between the Cu $2p_{3/2}$ and Cu $2p_{1/2}$ peaks is 20 eV, i.e. the same as for elemental copper.

Fig. 4 shows the Sb 4*d* spectra recorded for (Cu)[$Cr_{1.76}Sb_{0.16}\square_{0.08}$]$Se_4$ (the relevant spectra of the two other (Cu)[$Cr_{2-x-y}Sb_x\square_y$]$Se_4$ compounds are very much alike). For comparison, there are shown the Sb $4d_{5/2}$ and $4d_{3/2}$ doublets of the binary selenide $Sb_2Se_3$. Apparently, for all these compounds the spectra of the Sb 4*d* states are nearly same.

The characteristic Se *3d* spectra of the (Cu)[$Cr_{2-x-y}Sb_x\square_y$]$Se_4$ spinels are shown in Fig. 5. The splitting of the $3d_{5/2}$ and $3d_{3/2}$ doublets diminishes with increasing the Sb content. Moreover, the peaks move toward higher binding energy. The observed difference in their positions is about 0.6 eV, if the samples with the lowest and highest Sb concentration are compared.

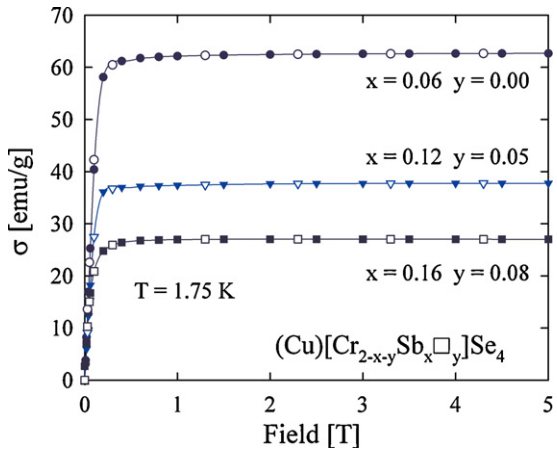


**Fig. 6.** Magnetic field variations of the magnetization in the (Cu)[$Cr_{2-x-y}Sb_x\square_y$]$Se_4$ single crystals, taken at a temperature of 1.75 K with increasing (closed symbols) and decreasing (open symbols) magnetic field strength.

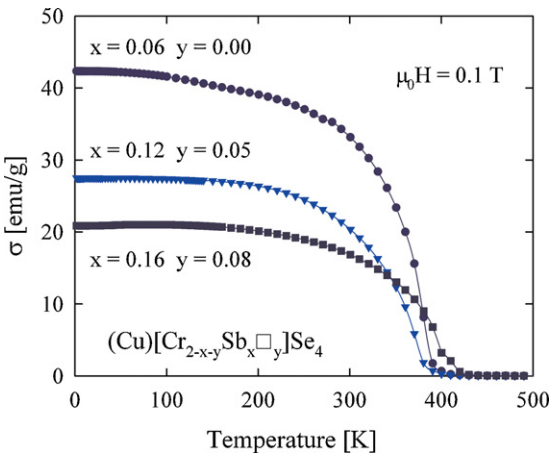


**Fig. 7.** Temperature dependencies of the magnetization in the (Cu)[$Cr_{2-x-y}Sb_x\square_y$]$Se_4$ single crystals, measured in an applied magnetic field of 0.1 T.

### 3.3. Magnetic properties

Fig. 6 presents the magnetization measured as a function of the magnetic field strength. For each compound, the $\sigma(H)$ variation shows a behaviour characteristic of soft ferromagnets, namely a rapid rise in the magnetization magnitude in weak fields is followed by a saturation in fields stronger than about 0.3 T. Apparently, the saturation magnetization $\sigma_s$ in the system distinctly decreases with increasing the Sb content. While $\sigma_s$ is equal to 62.7 emu/g for (Cu)[$Cr_{1.94}Sb_{0.06}$]$Se_4$, it drops to 37.8 emu/g for (Cu)[$Cr_{1.83}Sb_{0.12}\square_{0.05}$]$Se_4$, and eventually it decreases to only 27.0 emu/g in (Cu)[$Cr_{1.76}Sb_{0.16}\square_{0.08}$]$Se_4$. The corresponding saturation magnetic moment, calculated per single Cr ion, amounts to 2.82, 1.81 and 1.35 $\mu_B$, respectively. The former value is nearly identical with the chromium ordered magnetic moment in $CuCr_2Se_4$ determined from the neutron diffraction data [2,8]. The latter studies revealed a simple collinear ferromagnetic alignment of the magnetic moments localized on the trivalent Cr ions sites. Taking into account our XPS results, which definitively rule out any significant change in the valence state of chromium along the (Cu)[$Cr_{2-x-y}Sb_x\square_y$]$Se_4$ series, the observed distinct reduction in the magnitude of the saturation magnetic moment with increasing the Sb content might be attributed to the emergence and then gradual rise of the magnetic moment with the opposite orientation. Similar scenario was invoked before to rationalize the magnitude of the saturation magnetic moment in $CuCr_2Se_4$ which was smaller by about 1 $\mu_B$ per formula unit than 6 $\mu_B$ expected for two $Cr^{3+}$ ions [10–15]. In the case of (Cu)[$Cr_{2-x-y}Sb_x\square_y$]$Se_4$ the appearance of such antiparallel moments may naturally come up because of anticipated perturbations in the $Cr^{3+}$–Se–$Cr^{3+}$ superexchange interactions caused by disturbances in the lattice periodicity related not only to the presence of dopant Sb atoms yet also to the increasing number of vacancies.

As demonstrated in Fig. 7, the pronounced systematic variation in the magnitude of the saturation magnetic moment along the series (Cu)[$Cr_{2-x-y}Sb_x\square_y$]$Se_4$ are not accompanied by any distinct change in the value of the Curie temperature. For all three spinels the onset of the ferromagnetically ordered state is found slightly below 400 K, i.e. at a lower temperature than $T_c$ reported for the parent compound $CuCr_2Se_4$ [1]. The observed differences in the exact value of $T_c$ (defined as an inflection point on the $\sigma(T)$ curve) between the crystals studied do not exhibit any regular trend and therefore we do not attempt to drive any firm conclusion from this scatter. Here it seems worthwhile recalling a large spread in the $T_c$ value of nominally pure $CuCr_2Se_4$ (from 414.5 to 460 K [1,4–6]).

## 4. Conclusions

The single crystals of (Cu)[$Cr_{2-x-y}Sb_x\square_y$]$Se_4$ have been grown successfully for $x < 0.20$. This concentration of $Sb^{3+}$ does not affect the cubic close packed Se anionic sublattice. Although the $Sb^{3+}$ ions introduce a certain site disorder in the $Cr^{3+}$ subarray, they are not changing the electronic configuration $3d^3$ of the Cr ions, as evidenced by the magnitude of splitting of the Cr $2p_{3/2}$ core levels in XPS spectra. In consequence, no change in the magnitude of the chromium magnetic moment is expected. Therefore, the distinct reduction in the value of the saturation magnetization, revealed in the bulk magnetic measurements, should be attributed to a change in the magnetic structure of the compounds studied. A probable scenario seems the appearance of an antiparallel magnetic moment, whose amplitude scales with the number of defects (doped atoms, vacancies) in the crystal lattice. The ferrimagnetic component would thus be directly related to the expected perturbations in the $Cr^{3+}$–Se–$Cr^{3+}$ superexchange interactions. Obviously, to verify the latter hypothesis further experimental studies are indispensable, especially determination of the magnetic structures by neutron diffraction. Nevertheless, in the present context it is worth to recall that according to Refs. [47,48], further dilution of the Cr sublattice with Sb atoms results in a total frustration in the orientations of the localized magnetic moments, observed as spin-glass-like behaviour in the series of nonstoichiometric compounds $Cu_{1+x}Cr_{1.5+y}Sb_{0.5+z}Se_{4+t}$, where $-0.02 \le x \le 0.01$, $0.03 \le y \le 0.35$, $-0.2 \le z \le -0.02$ and $0.01 \le t \le 0.08$.

## Acknowledgment

This study was supported by the grant no. N N204 145938 from the Ministry of Science and Higher Education in Poland.

## Appendix A. Supplementary data

Supplementary data associated with this article can be found, in the online version, at doi:10.1016/j.jallcom.2011.10.048.

## References

[1] T. Kanomata, H. Ido, T. Koneko, J. Phys. Soc. Jpn. 29 (1970) 332–335.
[2] C. Colominas, Phys. Rev. 153 (1967) 558–560.
[3] I. Okońska-Kozłowska, J. Kopyczok, H.D. Lutz, Th. Stingl, Acta Crystallogr. C 49 (1993) 1448–1449.
[4] F.K. Lotgering, Proceedings of the International Conference on Magnetism, Nottingham (IOP, Bristol), 1964, p. 533.
[5] F.K. Lotgering, Solid State Commun. 2 (1964) 55–56.

[6] J.C. Th. Hollander, G. Sawatzky, C. Haas, Solid State Commun. 15 (1974) 747–751.
[7] I. Nakatani, H. Nosé, K. Masumoto, J. Phys. Chem. Solids 39 (1978) 743–749.
[8] D. Rodic, B. Antic, R. Rundlof, J. Blanusa, J. Magn. Magn. Mater. 187 (1998) 1448–1449.
[9] G.J. Snyder, T. Caillat, J.P. Fleurial, Mater. Res. Innovations 5 (2001) 67–73.
[10] J.B. Goodenough, Solid State Commun. 5 (1967) 577–580.
[11] A. Payer, M. Schmalz, R. Schöllhom, R. Schlögl, C. Ritter, Mater. Res. Bull. 25 (1990) 515–522.
[12] T. Saha-Dasgupta, M. De Raychaudhry, D.D. Sarma, Phys. Rev. B 76 (2007) 054441–54445.
[13] A. Kimura, J. Matsuno, J. Okabayashi, A. Fujimori, T. Shishidou, E. Kulatov, T. Kanomata, J. Electron Spectrosc. Relat. Phenom. 114–116 (2001) 789–793.
[14] A. Kimura, J. Matsuno, J. Okabayashi, A. Fujimori, T. Shishidou, E. Kulatov, T. Kanomata, Phys. Rev. B 63 (2001) 224420–224427.
[15] A. Deb, M. Itou, V. Tsurkan, Y. Sakurai, Phys. Rev. B 75 (2007) 024413–24416.
[16] F. Ogata, Y. Hamajima, T. Kambara, K.I. Gandaira, J. Phys. C: Solid State Phys. 15 (1982) 3483–3492.
[17] F.K. Lotgering, R.P. Van Stapele, Solid State Commun. 5 (1967) 143–146.
[18] J.B. Goodenough, J. Phys. Chem. Solids 30 (1969) 261–280.
[19] O. Yamashita, Y. Yamaguchi, I. Nakatani, H. Watanabe, K. Masumoto, J. Phys. Soc. Jpn. 46 (1979) 1145–1152.
[20] A. Winiarski, I. Okońska-Kozłowska, J. Heimann, M. Neumann, J. Alloys Compd. 232 (1996) 63–66.
[21] T. Groń, K. Bärner, Ch. Kleeberg, I. Okońska-Kozłowska, Physica B 225 (1996) 191–196.
[22] K.P. Belov, L.I. Koroleva, A.I. Kuzminykh, I.V. Gordeev, Ya.A. Kessler, A.V. Rozantsev, Phys. Lett. A 94 (1983) 235–238.
[23] T. Groń, S. Mazur, H. Duda, J. Krok-Kowalski, E. Malicka, Physica B 391 (2007) 371–379.
[24] H. Duda, E. Maciążek, T. Groń, S. Mazur, A.W. Pacyna, A. Waśkowska, T. Mydlarz, A. Gilewski, Phys. Rev. B 77 (2008) 035207–35208.
[25] E. Maciążek, H. Duda, T. Groń, T. Mydlarz, A. Kita, J. Alloys Compd. 442 (2007) 183–185.
[26] T. Groń, E. Maciążek, J. Heimann, J. Kusz, I. Okońska-Kozłowska, K. Bärner, Ch. Kleeberg, Physica B 254 (1998) 84–91.
[27] E. Maciążek, A. Molak, T. Goryczka, J. Alloys Compd. 441 (2007) 222–230.
[28] I. Jendrzejewska, T. Mydlarz, I. Okońska-Kozłowska, J. Heimann, J. Magn. Magn. Mater. 186 (1998) 381–385.
[29] T. Groń, A. Krajewski, H. Duda, P. Urbanowicz, Physica B 373 (2006) 245–252.
[30] E. Malicka, T. Groń, D. Skrzypek, A.W. Pacyna, D. Badurski, A. Waśkowska, S. Mazur, R. Sitko, Philos. Magn. 90 (2010) 1525–1541.
[31] M. Hamedoun, R. Masrour, K. Bouslykhane, A. Hourmatallah, N. Benzakour, J. Magn. Magn. Mater. 320 (2008) 1431–1435.
[32] R. Sitko, B. Zawisza, E. Malicka, Spectrochim. Acta, Part B 64 (2009) 436–441.
[33] Oxford Diffraction 2005, CrysAlis CCD. Data Collection Software, Oxford Diffraction Ltd., Wrocław, Poland.
[34] Oxford Diffraction 2008, CrysAlis RED. Data Reduction program. Issue 171.32.6, Oxford Diffraction Ltd.
[35] G.M. Sheldrick, Acta Crystallogr. 11 (2008) 2–122, A64.
[36] R.D. Shanon, Acta Crystallogr. 75 (1976) 1–767, A32.
[37] I.D. Brown, D. Altermatt, Acta Crystallogr. 24 (1985) 4–247, B41.
[38] N.E. Brese, M. O'Keeffe, Acta Crystallogr. 19 (1991) 2–197, B47.
[39] I.D. Brown, Acta Crystallogr. 55 (1992) 3–572, B48.
[40] I.D. Brown, J. Appl. Crystallogr. 29 (1996) 479–480.
[41] V. Tsurkan, St. Plogmann, M. Demeter, D. Hartmann, M. Neumann, Eur. Phys. J. B 15 (2000) 401–403.
[42] E. Malicka, A. Waśkowska, J. Heimann, T. Mydlarz, R. Sitko, D. Kaczorowski, J. Solid State Chem. 181 (2008) 1970–1976.
[43] A. Ślebarski, M. Neumann, B. Schneider, J. Phys.: Condens. Matter 13 (2001) 5515–5518.
[44] E.S. Ilton, W.A. de Jong, P.S. Bagus, Phys. Rev. B 68 (2003) 125106–125108.
[45] Handbook of X-Ray photoelektron spectroscopy, Physical Electronics (1992).
[46] X. Chen, X. Wang, C. An, J. Liu, Y. Qian, J. Cryst. Growth 256 (2003) 368–376.
[47] J. Krok-Kowalski, J. Warczewski, H. Duda, P. Gusin, K. Krajewski, T. Śliwińska, A. Pacyna, T. Mydlarz, E. Malicka, A. Kita, J. Alloys Compd. 430 (2007) 39–42.
[48] J. Krok-Kowalski, J. Warczewski, P. Gusin, T. Śliwińska, T. Groń, G. Urban, R. Rduch, G. Władarz, H. Duda, E. Malicka, A. Pacyna, L.I. Koroleva, J. Phys.: Condens. Matter 21 (2009) (5pp) 035402.